Mon. Not. R. Astron. Soc. **263,** 628–640 (1993)

# The nature of star formation in lensed galaxies at high redshift

Ian Smail,[1]★ Richard S. Ellis,[1] Alfonso Aragón-Salamanca,[1] Genevieve Soucail,[2] Yannick Mellier[2] and Edmond Giraud[3]

[1] *Physics Department, University of Durham, South Road, Durham DH1 3LE*
[2] *Observatoire de Toulouse, avenue Édouard Belin, F-31400 Toulouse, France*
[3] *Centre de Physique Theorique, CNRS Luminy, F-13288 Marseille Cedex 9, France*

Accepted 1993 January 27. Received 1992 December 3; in original form 1992 May 5

## ABSTRACT

We present near-infrared photometry of all available gravitationally lensed 'arcs' with spectroscopic redshifts. By combining this photometry with optical data, we find that the bulk of the systems with $z \sim 1$ are intrinsically blue across the rest-frame spectral region 2000 Å to 1 μm. Using a combination of optical and optical–infrared colours, we demonstrate that these systems cannot be blue by virtue of a secondary burst of star formation superimposed on an evolved population, but we are unable to distinguish directly between major star formation events in a generic young galaxy and an extended era of constant star formation typical of late-type spirals. Using various arguments, we conclude that our arcs represent modest gravitational magnification of typical field galaxies. Consequently, if the star formation seen is representative of that in field galaxies at $z \geq 1$, the absence of high-redshift galaxies in current deep spectroscopic surveys to $b_J \simeq 24$ supports the hypothesis that the bulk of the star formation in normal galaxies occurred over an extended era up to the epoch corresponding to $z \sim 1$.

**Key words:** galaxies: evolution – galaxies: formation – galaxies: photometry – cosmology: observations – gravitational lensing – infrared: galaxies.

## 1 INTRODUCTION

From an observational perspective, the most useful feature of gravitational lensing occurs when the potential well of a foreground cluster of galaxies distorts and magnifies the image of a distant galaxy into a giant arc. The distortion provides an easily identifiable signature which may be used to select preferentially objects at high redshift. Moreover, since the lensing process conserves surface brightness, the resulting magnification enables information to be gathered about the dynamics and spectral colour of a distant galaxy on spatial scales normally unattainable.

There has been a steady increase in the number of spectroscopically confirmed giant arcs (see Soucail 1992 for a recent update). However, these are largely serendipitous discoveries, and do not yet constitute a complete sample. To overcome this problem, Smail et al. (1991) undertook a survey of 20 clusters to search for arcs, maintaining a constant surface brightness limit for their detection. This survey indicated that giant arcs (i.e. those bright enough for spectroscopy with telescopes of the 4-m class) are rather rare. Nevertheless, since the lensed sources *must* be reasonably distant, even a small sample will be useful, complementing data on field galaxies derived from magnitude-limited redshift surveys (Colless et al. 1990, 1993; Cowie, Songaila & Hu 1991). Indeed, although such surveys now reach $b_J \sim 24$, the median depth is only $\bar{z} \sim 0.4$: few galaxies are found with $z > 1$. Furthermore, for many applications in galaxy evolution, precise redshifts are not required: it would be sufficient to know the bulk properties of sources lying substantially beyond the distance of the lensing cluster.

An important motivation for this paper is the observation (Fort 1990; Mellier et al. 1991) that most of the spectroscopic arcs have optical colours similar to the *flat-spectrum* blue galaxies which dominate the faint field population. If correct, a careful study of a few arcs might reveal the nature and origin of this puzzling population. However, we must be aware of the possible role of selection effects in the apparent pre-eminence of blue arcs in the sample. A bias may arise from the preferential selection of unrepresentative blue star-forming galaxies by virtue of their high surface brightness (Phillipps, Davies & Disney 1990). Since lensed galaxies are essentially identified to a limiting surface brightness, it is also conceivable that only the high surface brightness peaks of galaxies would be detected.

When observing high-redshift galaxies for the purposes of constraining evolutionary models, the three most useful

★ Present address: CalTech 105-24, Pasadena, CA91125, USA.

parameters to measure are the stellar mass, and the current and time-averaged star formation rates. A comparison of the latter two parameters may indicate whether we are witnessing a galaxy in an important phase of its lifetime, e.g. during a major episode of star formation, or whether the star formation is continuous in time. In this paper we will examine the colours of the giant arcs across a wide wavelength range, extending Mellier et al.'s study to infrared wavelengths. At $z \sim 1$ the $K$ band samples rest-frame wavelengths of $\lambda \sim 1$ μm, whereas the optical colours sample the rest-frame UV. For conventional initial mass functions (IMFs) and stellar populations older than a few $\times 10^8$ yr, the major fraction of the 1-μm radiation comes from stars that are on either the main sequence or the red giant branch, the progenitors of the latter group being long-lived main-sequence stars (Buzzoni 1989). In a 0.5-Gyr population, the contributions to the 1-μm light are main-sequence stars (30 per cent), core He burning stars (30 per cent) and asymptotic giant branch stars (40 per cent) (Bruzual & Charlot 1992). The $K$-band flux therefore gives a better indication of the long-term star formation rate (and hence, indirectly, the stellar mass of the galaxy) than do the optical colours which measure the instantaneous star formation rate, since the UV flux is dominated by hot, young stellar populations. The combination of optical *and* optical–infrared colours is thus particularly effective in addressing the nature of the star formation seen in these distant sources.

A plan of the paper follows. In Section 2 we discuss the role that selection biases may play in terms of optical and optical–infrared colours, and demonstrate the important role which infrared photometry plays in the resolution of such questions. In Section 3 we review the observational material and present new infrared images and photometry for the sample under consideration. The optical–infrared colours are presented and discussed in Section 4, where we also discuss spatially resolved photometric information for individual cases. Finally, we discuss in Section 5 the implications in the general context of the faint galaxy populations, and present our main conclusions in Section 6.

## 2 OPTICAL AND INFRARED SELECTION EFFECTS

It is well known that star-forming galaxies are more readily visible in optical surveys to modest redshifts. This selection bias occurs because the rest-frame ultraviolet (dominated by light from hot young stars) is redshifted into the observing passband. Although the blue colour of many of the arcs discussed in Mellier et al. (1991) indicates sources with a population of young stars, the implications for galaxy evolution are unclear. Data that sample the rest-frame UV cannot distinguish, for example, between a massive spiral galaxy with continuous star formation and a less massive galaxy undergoing a more intense, but short-lived, burst of star formation.

The distinction is important to resolve because deep redshift surveys (Colless et al. 1990, 1993) find that the bulk of the faintest blue field galaxies are at surprisingly modest redshifts, $z \sim 0.3$–$0.5$. It has been argued that these are *not* the evolving precursors of $L^*$ galaxies (Cowie et al. 1991; Babul & Rees 1992), but are an entirely independent dwarf population. Alternatively, Broadhurst, Ellis & Glazebrook (1992) have suggested that such star-forming low-luminosity sources at moderate redshift evolve via merging to form the present-day population of massive galaxies. In either case, independent data from lensing studies on systems at $z \simeq 1$ would be highly valuable.

In examining an optically blue arc, the critical question is whether we are witnessing a highly magnified dwarf made temporarily luminous by an intense burst of star formation, a system undergoing its first major period of star formation, or the precursor of a massive $\simeq L^*$ galaxy whose star formation rate is changing more slowly. In the final model, the arcs could be representative of present-day massive late-type spirals whose properties can be modelled rather well via a continuous star formation rate (SFR).

To illustrate the role that infrared photometry can play in differentiating between these possibilities, we examine in Fig. 1(a) the optical and optical–infrared colour evolution of a model galaxy undergoing star formation changes of the kind discussed above. For convenience in later discussion, we present this in terms of colours viewed with our standard passbands at a redshift of $z = 1$. The calculations were made using Bruzual and Charlot's most recent evolutionary code (Bruzual & Charlot 1992). Their new models follow in detail all the relevant stages of stellar evolution, including the red and asymptotic giant branches and the post-AGB stage. These authors claim that the models correctly reproduce the colours of stellar populations from the UV to the near-IR over a broad range of ages. They can be computed for an arbitrary star formation history. A standard Salpeter (1955) IMF with an upper mass limit of 125 $M_\odot$ was used.

First, we consider a family of primaeval galaxies undergoing their first major star-forming episode. In each case, the burst is of 1-Gyr duration and is arranged to occur 0.2–5.0 Gyr before $z = 1$ (we adopt $H_0 = 50$ km s$^{-1}$ Mpc$^{-1}$, $q_0 = 0.5$ throughout). The second family of models has the added feature of a secondary instantaneous burst of star formation comprising 10 per cent of the total gas + stellar mass, occurring 0.2–5.0 Gyr before $z = 1$. This burst is superimposed upon an older ($\simeq 5$ Gyr) evolved population. Finally, we plot the locus of a galaxy with a constant star formation rate, and with a formation epoch 0.2–0.5 Gyr prior to $z = 1$. All three models contain a phase during which the galaxy is very blue in $B-R$, i.e. optical colours alone cannot differentiate between the very different scenarios.

However, the figure shows that the addition of the optical–infrared colour $R-K$ allows a clear discrimination between the burst models in the range of interest. This is primarily because the $K$ light is sensitive to the longer term star formation rate. Only a secondary burst model seen immediately after a short intense burst can become as blue in $R-K$ as the primaeval model. Thus the $(B-R,\ R-K)$ colour plane offers a straightforward way to estimate the contribution that recent star formation may have made to the optical colours. No assumptions need be made about the structural state of the source. The distinction between a secondary-burst model and a constant-SFR model is also clear in $R-K$, but it is much harder to differentiate between a 'single-burst' galaxy viewed close to its formation and the constant-SFR case. Fig. 1(a) shows, none the less, that, to obtain a representative view of the stellar populations of the distant arc sample discussed by Mellier et al. (1991), near-infrared photometry will be particularly valuable.

## 3 OBSERVATIONS AND DATA REDUCTION

Our sample consists of those available giant arcs with either spectroscopic redshifts or redshift constraints from spectral information; the complete list and the sources of our photometry are summarized in Tables 1 and 2. Our strategy has been to use 2-μm $K$-band photometry taken with an infrared array in conjunction with optical CCD photometry in $B$ and $R$, some of which was published by Mellier et al. (1991). Although in certain cases the spectral data are inconclusive, those arcs have been included where the case for lensing is particularly convincing, since they increase the sample size. Such cases are discussed individually.

The crowded cluster fields and the poor contrast of the faint arcs against the cluster members, especially in the $K$ band, make measurement of 'total' arc magnitudes very difficult because of contamination problems. We have chosen therefore to measure aperture magnitudes in $K$ and to use associated aperture photometry at shorter wavelengths to compute the colours. Ideally, we would prefer to measure a total $K$ magnitude in order to estimate the intrinsic luminosity of the arc. However, as the magnification factors associated with the gravitational lensing are somewhat model-dependent (Hammer 1991), a more realistic approach which we adopt is to measure an average surface brightness for each arc and to use this in conjunction with an assumed angular size and redshift to calculate the luminosities.

The new data consist of deep $K$-band images obtained with the 3.8-m UK Infrared Telescope (UKIRT) on Mauna Kea, using the 58×62 InSb array IRCAM (McLean et al. 1985). IRCAM offers a choice of three pixel scales (0.62, 1.24 or 2.4 arcsec pixel$^{-1}$). Since the data were taken over a series of runs, occasionally during allocations made to other programmes, we used one of the two smaller scales (see Table 1 for details). Although the 0.62 arcsec pixel$^{-1}$ scale is best matched to the seeing, allowing more accurate photo-

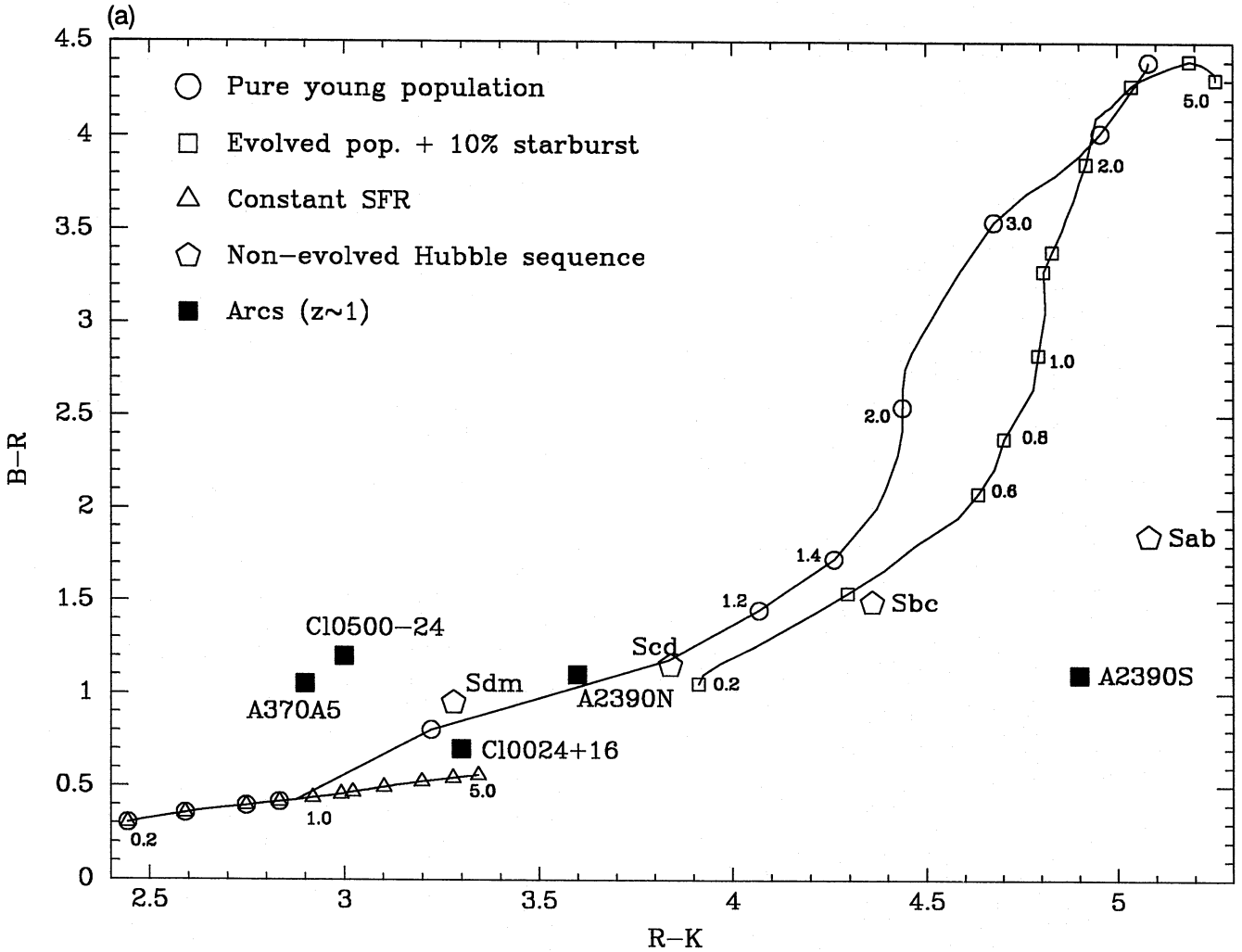


**Figure 1.** (a) $(B-R)$-$(R-K)$ diagram for galaxies viewed at $z=1$ according to three different star formation histories. The tracks refer to a family of galaxies whose burst of star formation occurred at different times *before* $z=1$. The symbols on the curves mark the starting times: the first is for 0.2 Gyr before $z=1$, and they are then positioned every 0.2 Gyr until 1.4 Gyr, and after that every 1 Gyr from 2 to 5 Gyr. 'Pure young population' objects suffered their initial 1-Gyr burst as indicated. The superimposed burst models consist of an older (5 Gyr) population, which encounters a secondary instantaneous burst involving 10 per cent of the stellar mass at the given time prior to $z=1$. The final model is a constant star formation model with a variable formation epoch. The present-day Hubble sequence as observed at $z=1$ is also shown. Data points refer to high-redshift arcs; the northern and southern sections of Abell 2390 are plotted separately.

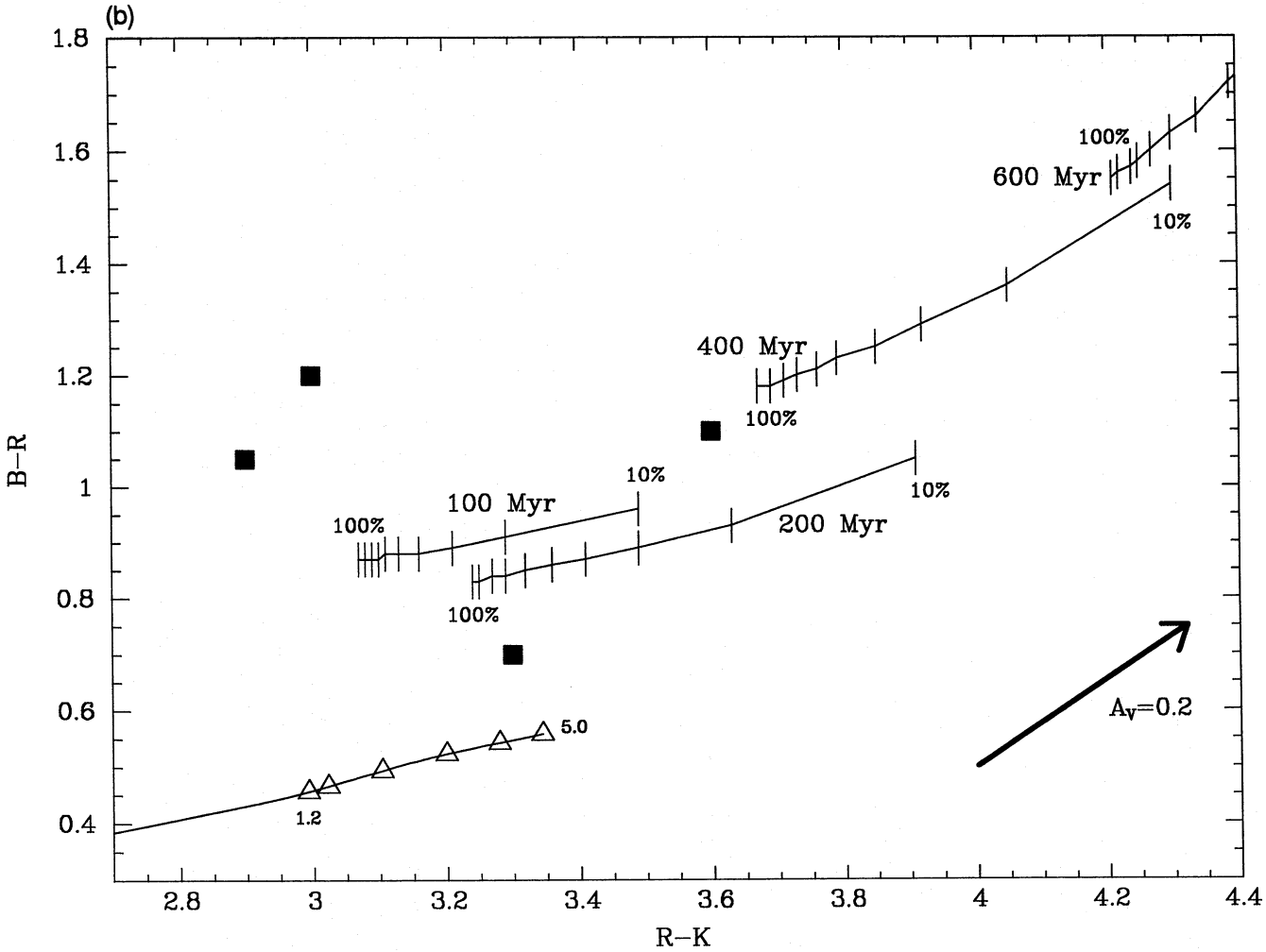


**Figure 1.** (b) $(B-R)$-$(R-K)$ diagram as in (a), but showing the tracks of different burst fractions for a given age in the secondary-burst model. The remainder is comprised of an evolved population as above. The separate curves correspond to bursts occurring at the stated times before $z=1$; the increments show the fraction of the stellar mass of the system created in the burst (from 10 to 100 per cent in 10 per cent steps). The 100-Myr track is heavily influenced by individual stellar evolution phases in the instantaneous burst. Also plotted using the same symbols as in (a) are the observations of the giant arcs, the continuous star formation track and the extinction vector for solar-abundance dust.

**Table 1.** The giant-arc sample.

| Arc | $\alpha$ (1950.0) | $\delta$ (1950.0) | $z_{cl}$ | $z_{arc}$ | $T_{exp}$ |
|---|---|---|---|---|---|
| Cl0024+16 | 00 23 58.5 | +16 52 51 | 0.39 | >1.[1] | 11760 |
| A370 A0 | 02 37 20.4 | -01 47 51 | 0.375 | 0.725[2] | 6120 |
| A370 A5 | 02 37 20.8 | -01 48 15.8 | 0.375 | 1.308[1] | 12420 |
| Cl0500-24 | 04 59 02.1 | -24 29 18 | 0.321 | 0.913[3] | 11700 |
| A963 N | 10 13 58 | +39 17 18 | 0.206 | 0.771[4] | 14720 |
| A2390 | 21 51 15.5 | +17 27 51 | 0.230 | 0.913[5] | 10720 |
| Cl2244-02 | 22 44 38.3 | -02 21 30.0 | 0.329 | 2.238[1] | 16320 |

Spectroscopy references: [1]Mellier et al. (1991); [2]Soucail et al. (1988); [3]Giraud (1992); [4]Ellis, Allington-Smith & Smail (1991); [5]Pelló et al. (1991).

metry in the crowded cluster environments, the field of view is then restricted, especially when using in-field 'dithering' methods (cf. Cowie et al. 1988) to flat-field the data. In some cases, more than one arc could be secured with a wider field, making it profitable to use a larger pixel scale.

The in-field dithering technique constructs a sky flat-field for a particular field from a number of disregistered object frames taken in sequence. Flat-fielding has to be performed to high precision to detect the very low surface brightness arcs against the bright sky in $K$. The number of frames used in this process depends upon the unit exposure time, but was usually $\simeq 8$–9. Each frame was dithered on a rectangular $3\times 3$ grid with $\geq 5$-arcsec spacing. This method allows maximum on-source integration whilst providing a coeval flat-field – which is especially important in the near-infrared, since the spatial structure of the sky emission varies on a time-scale of minutes. In crowded fields, we occasionally implemented the alternative procedure of using separate offset sky-flats interleaved with the object frames (Aragón-Salamanca, Ellis & Sharples 1991). Here, the exposure times depended upon the observing conditions, but were typically $\simeq 40$ s for background-limited operation at the 0.62 arcsec pixel$^{-1}$ scale.

Both sky and object frames were linearized and dark-subtracted, and bad pixels were removed by interpolation. Flat-fielding was accomplished by dividing each object frame by the scaled sky-flat frame (see above). The flat-fielded

image frames were registered using fractional pixel shifts and median-combined to remove cosmic ray events. All reduction was carried out on the Durham node of Starlink using IRCAM and purpose-written software.

The in-field dithering technique produces the most impressive results, penetrating to fainter surface brightness limits than those quoted in earlier work (cf. Aragón-Salamanca 1991). In a 3.3-h dithered exposure, we obtain virtually photon-noise-limited performance, a flatness of better than 4 parts in $10^5$ and a 1 $\sigma$ surface brightness limit of $\mu_K = 23.5$ mag arcsec$^{-2}$. Representative $K$ images are reproduced, along with deep multicolour optical CCD frames, in Fig. 2 (opposite p. 632).

Calibrations were obtained via defocused exposures of bright standard stars taken from the list of Elias et al. (1982). These were interspersed with the observations and reduced using similar procedures. Photometry was performed using large synthetic apertures, to give zero-points for each night independently. Photometric comparisons from repeat observations on different nights and between runs indicate zero-point errors $< 0.05$ mag.

One arc (Cl 0500 − 24) was observed through a $K'$ filter, the long-wavelength edge of which is curtailed to reduce the rising thermal background across the passband. The effective wavelength is $\lambda_{\rm eff} \sim 2.1$ μm. To reduce this measurement on to the standard $K$ system, colour relations were calculated from standard stars with a wide range of $H-K$ colours and from the infrared colours of different galaxy classes, using the known filter transmissions. A linear relation, $K' = K - 0.2(H-K)$, was deduced and, for the arc in question, we assumed $H-K = 0.8$ for the transformation. Since this $H-K$ value is representative of all morphological types beyond $z \sim 0.6$, the uncertainty in the transformation should be small.

Before measuring magnitudes within fixed apertures, the optical frames were resampled to the larger infrared pixel scale, rotated and aligned. Images were also smoothed when there were significant differences in the seeing conditions amongst the various filters. This latter step produces only a small correction to the actual colours, and the uncertainty is incorporated in our formal photometric error.

Aperture sizes and background-subtraction techniques were chosen on an individual basis for each arc. Several arcs (those in Cl 0017 − 20, Cl 0024 + 16, Abell 370 A5 and Cl 0500 − 24) are relatively uncontaminated by cluster members, and photometric measures were taken inside the faintest isophote that was unaffected by other objects. Other arcs, however (e.g. in Abell 2390), are merged with a bright cluster galaxy. In these cases, the contaminating light was removed by assuming symmetry in the contaminating galaxy. A copy of the frame was rotated, recentred and subtracted from the original to remove the galaxy. The final frame was then inspected to determine if the subtraction had successfully removed the galaxy image. Other arcs (e.g. in Abell 370 A0) have projected sources superimposed, and here colours were measured in all uncontaminated regions, on a pixel-by-pixel basis. The most critical cases are the arcs in Cl 2244 − 02 and Abell 963, which are embedded in the haloes of several galaxies. To measure colours for these, we calculated the halo contribution in the appropriate aperture by interpolation. Systematic sources of photometric error are, of course, a concern, and there may be unresolved contaminating sources with colour quite different from the arcs. In a few cases, the $K$ light is sufficiently faint that a small error in sky subtraction might produce a significant change in the optical–infrared colour. Rather than make general statements about the precision achieved, we discuss uncertainties for individual cases in Section 4. For the brighter arcs, it is also possible to measure colours as a function of spatial position along the arc. This provides important additional information, for example on the lensing configurations.

Although our optical data are often taken from the frames analysed by Mellier et al. (1991), we have reduced these completely independently. A comparison of our $B-R$ colours with those of Mellier et al. shows good agreement within our quoted errors, with the exception of Abell 2390, for which our $B-R$ colour is significantly bluer. In this particular arc, there is a strong optical–infrared colour gradient but no gradient in $B-R$. This disagreement cannot then be attributed to the use of different apertures. We return to this problem in Section 4.2. Our photometric results are summarized in Table 2.

Finally, we report the discovery of the first near-infrared-selected arc. The deep $K$ image of Cl 2244 − 02 reveals a second, shorter arc further from the cluster centre, with a similar radius of curvature to the giant arc. This detection prompted the acquisition of a much deeper $B$ image, which shows the second arc at a surface brightness of $\mu_B = 27.6$ mag arcsec$^{-2}$. The optical detection suggests that the Lyman limit has not reached the $B$ band, and thus that $z < 3.8$. Although this arc appears blue in the optical ($B-R \leq 1$), in contrast to the main sample it is prominent in $K$ and hence very red in the optical–infrared region ($B-K = 7.3$ and $R-K \geq 6.3$). An early-type galaxy placed at the redshift of the cluster ($z = 0.329$) has $B-K \sim 6.2$ and would have $B-K = 7.3$ at $z \sim 0.6$, when $R-K = 4.3$. However, the unusual feature of the arc is the faintness in $R$ – the limits imposed by this in $R-K$ require the source to have $z \geq 1.2$, and the $B-R$ value would then reflect a strong up-turn in the spectral energy distribution (SED) below 2000 Å. The other alternative is that the bright $K$ magnitude is a result of strong line emission in that passband. However, the arc is sufficiently faint, especially in the optical, that these colours must be viewed with some caution. In the deep high-resolution $B$ data, the second arc is approximately 10 arcsec long and is unresolved.

A very simple geometrical lensing model suggests that the second arc could be at least as distant as the primary arc, and possibly even further away. The colours are consistent with those expected for either an E/S0–Sab galaxy with a strong UV up-turn, or a system with very strong H$\alpha$ observed at the redshift of the primary arc; in this case the source would be luminous, with $M_K \sim -25.7$. The red optical–infrared colour

**Table 2.** Photometric results.

| Arc | B−R | R−K | B−K | $\mu_K$ | $M_K$ |
|---|---|---|---|---|---|
| Cl0024+16 | 0.7[1] | 3.3±0.1 | 4.0 | 21.7 | -22.1 |
| A370 A0 | 1.97[2] | 4.1[3] | 6.1 | 18.5 | -24.1 |
| A370 A5 | 1.05[4] | 2.9±0.2 | 3.9 | 21.6 | -22.1 |
| Cl0500-24 | 1.2[5] | <3 | <4.2 | >22.0 | <-21.1 |
| A963 N | 0.7±0.3 | 2.7±0.3 | 3.4 | 22.0 | -20.8 |
| A2390 | 1.1±0.1 | 4.6±0.1 | 5.7 | 20.0 | -23.1 |
| Cl2244-02 | 1.0±0.1 | 2.5±0.2 | 3.5 | 21.8 | -22.8 |

Photometry references: [1]Koo (1988); [2]Fort et al. (1988); [3]Aragón-Salamanca & Ellis (1990); [4]Hammer et al. (1989); [5]Pelló et al. (1991).

Opposite p. 632, MNRAS, **263**

(a)

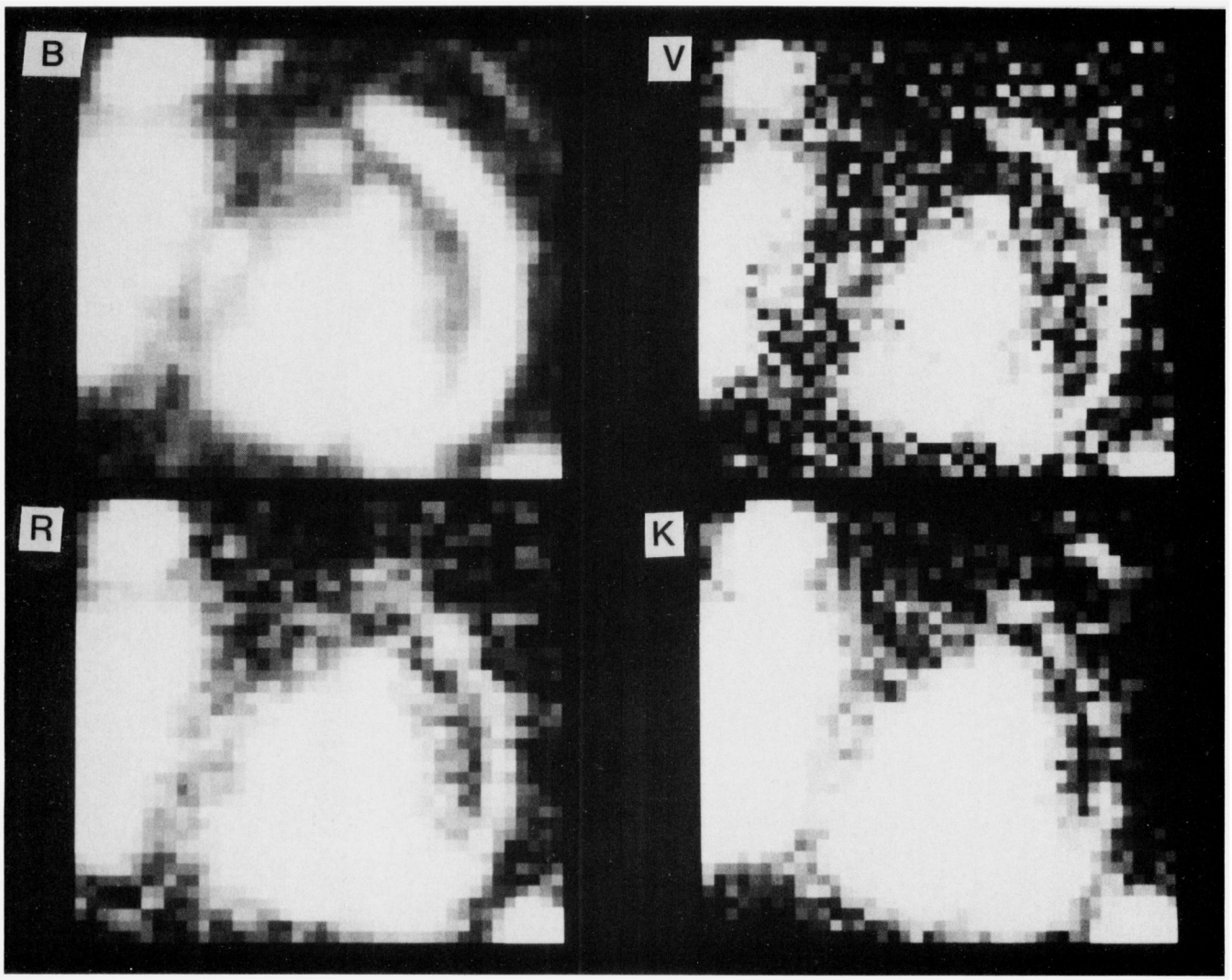


**Figure 2.** Broad-band images of selected arcs in our sample. North is at the top, east is to the left. (a) *BVRK* images of Cl 2244 − 02; the giant arc is clearly detected in the *K* image. The second infrared arc is concentric with the giant arc and north-west of it. The vast difference in the colours of the arcs can be seen by comparing the *B* and *K* images. The frames are $25 \times 25$ arcsec$^2$. (b) *BRK* and $B-K$ images of Abell 2390. The images are $29 \times 27$ arcsec$^2$. The $B-K$ image was constructed by scaling the two images to remove the cluster ellipticals, and shows the strong colour gradient along the arc.

(b)

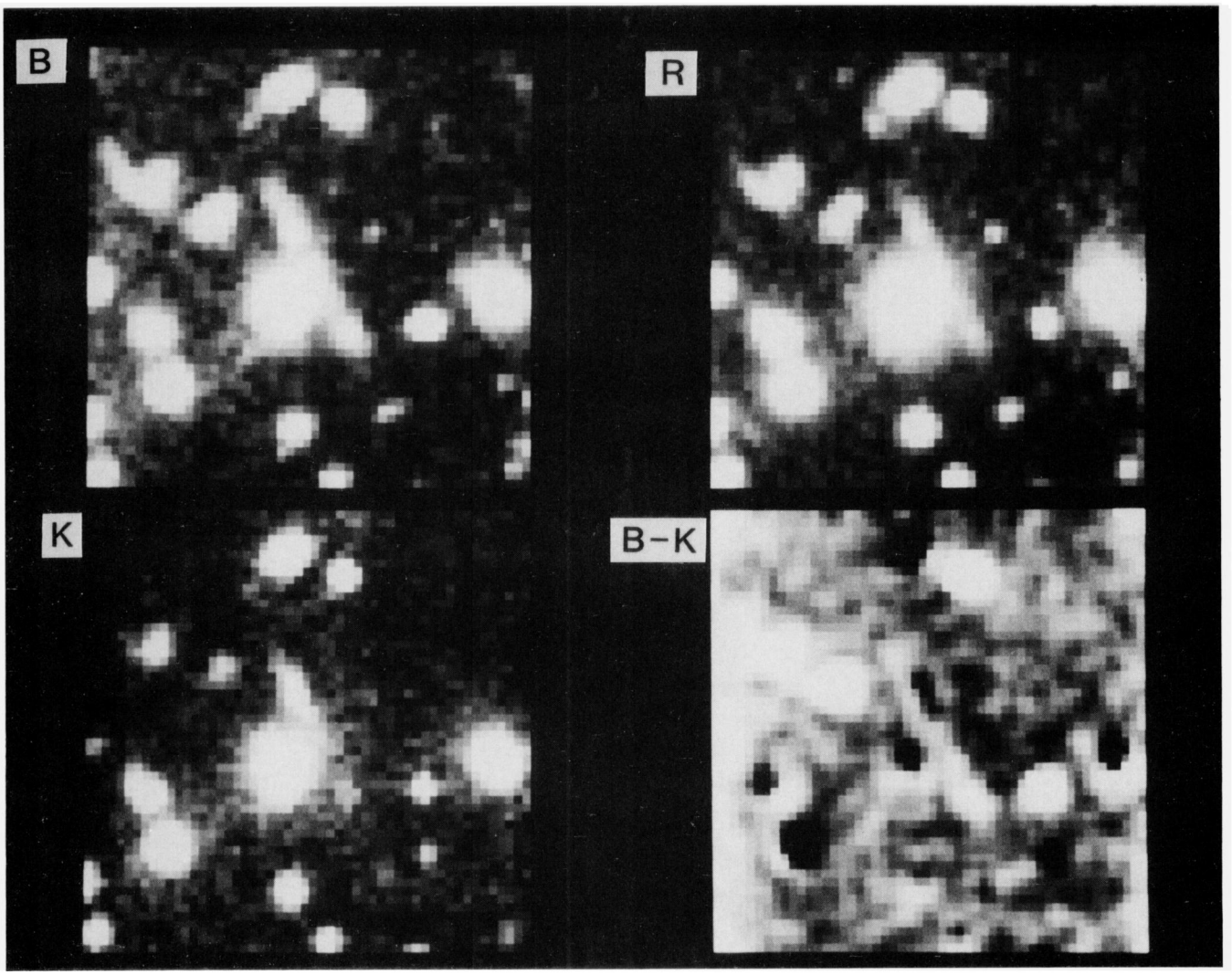


**Figure 2** – *continued*

is important, however, in view of the near-uniform optical–infrared colours for the optically selected arcs, a point we return to below.

## 4 PHOTOMETRIC RESULTS FOR DISTANT GALAXIES

### 4.1 Broad-band colours and SEDs

In Fig. 3 we plot the observed $B-R$, $R-K$ and $B-K$ colours versus redshift for our sample. For comparison, we also plot $B-R$ versus redshift as measured by Colless et al. (1990, 1993) for their samples of faint field galaxies with $21 < b_J < 24$. At the limit probed with the spectroscopic samples, objects are found with colours as red as present-day ellipticals to $z \sim 0.5$. However, the important point, originally noted by Fort (1990), is that *both* data sets include objects with very blue optical colours ($B-R \leq 1$) typical of the most extreme star-forming Sm/Irr galaxies present today (e.g. NGC 4449). Interestingly, for the arcs there is a distinctive trend to bluer colours with higher redshift, although the sample is obviously rather small. It would appear therefore that the arcs sample a population of galaxies whose star formation activity at $z \sim 1$ is much more vigorous than both a random cross-section of the present Hubble sequence and (possibly) the lower redshift field galaxies in somewhat brighter surveys.

In Fig. 3(c) we compare the data with the colours of the faint field galaxies in the recent survey of Cowie et al. (1991) limited at $B \leq 24$. It has been suggested that the latter sources, whose spectra show strong [O II] emission, are dwarf galaxies undergoing disruptive star formation or merging to form the present-day galaxy population (Babul & Rees 1992; Broadhurst et al. 1992). The similarity in colours is striking, emphasizing the importance of the $K$-band measurements as

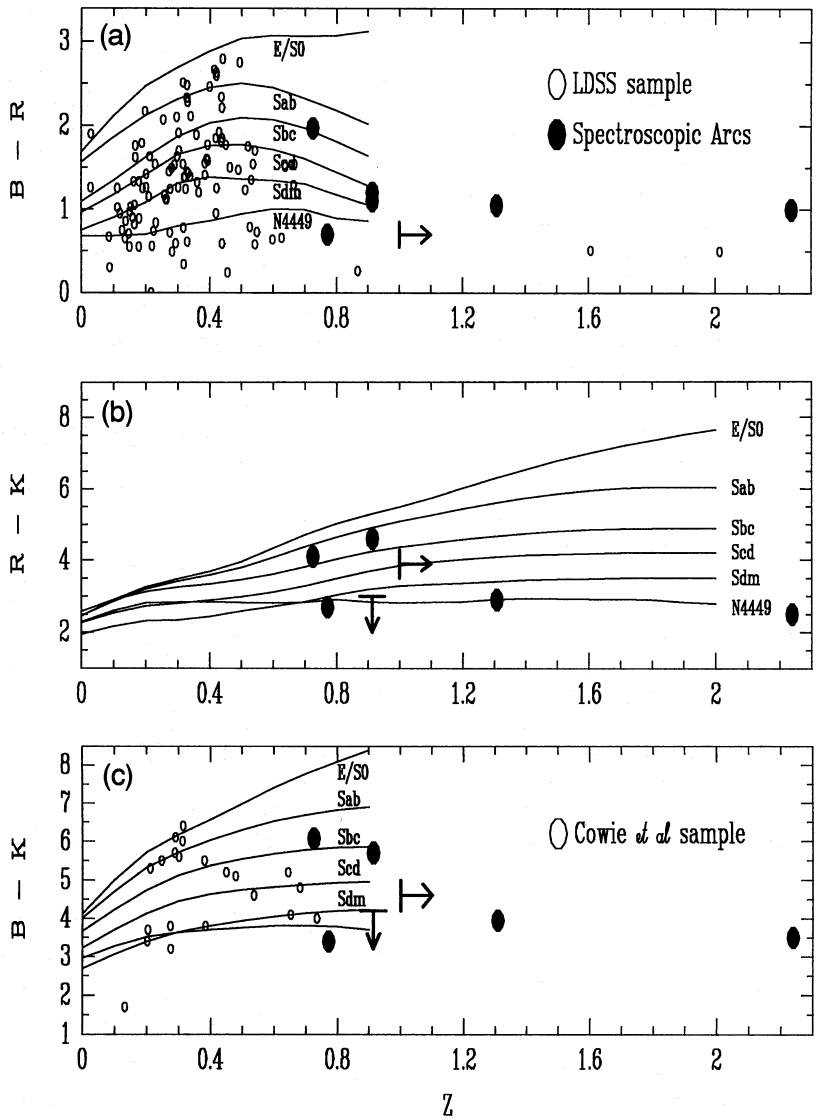


**Figure 3.** (a) $B-R$ versus redshift for the arc sample (●) compared to the distribution of $B-R$ for the Colless et al. (1990, 1993) samples of faint field galaxies (○). The horizontal arrow shows the probable redshift range of Cl 0024 + 16. (b) $R-K$ colour versus redshift for the arc sample. The vertical arrow denotes the upper limit for the arc in Cl 0500 + 24, converted from $K'$ to $K$. (c) $B-K$ colour versus redshift for the arc sample compared to the colours of field galaxies in the faint optical survey of Cowie et al. (1991) (○). Curves denote the expected colours of the non-evolving Hubble sequence.

well as the need to estimate the lensing magnification so that the $K$ luminosities can be derived.

In Section 2 we demonstrated how optical colours can mislead at high redshift because of biases introduced by ultraviolet flux which enters the optical region. Indeed, several of the arcs with $z<1$ that are blue in $B-R$ turn out to have fairly reasonable colours in $R-K$, indicative of precisely this effect. Only a small amount of additional star formation in a normal spiral would be needed to explain the combined *BRK* colours. More interestingly, however, the four arcs claimed to be the most distant of all – Abell 370 A5 ($z_{\rm arc}=1.3$), Cl 0500−24 ($z_{\rm arc}=0.913$), Cl 2244−02 ($z_{\rm arc}=2.24$) and Cl 0024+16 ($z_{\rm arc}>1$) – are also blue in $R-K$.

We plot the colours of the most distant arcs on the $B-R$ versus $R-K$ diagram in Fig. 1(a). *The most striking conclusion is the clear demonstration that the four arcs with $z\geq 0.9$ are not readily explained by models incorporating subsidiary starbursts of a short-term nature superimposed on a pre-existing stellar population.* We are witnessing either constant star formation in late-type galaxies, or a significant burst of star formation in a genuinely young population.

To quantify this statement, we have plotted in Fig. 1(b) the colours of a family of secondary burst models as a function of the fraction of mass in the second burst. Each curve is for an instantaneous burst occurring at the given time before $z=1$, the remaining fraction of the system being composed of an evolved population. Given the instantaneous nature of the burst, the 100-Myr locus is strongly affected by individual stellar evolution phases, and should be taken as illustrative only. Nevertheless, the older tracks show that agreement with the arc colours can only be achieved by viewing the system very soon after the burst occurred. The earliest burst that could reasonably explain all of the arc colours needs to occur less than 400 Myr before $z=1$, and would have to create at least 50 per cent of the stellar mass of the system. Later bursts allow smaller mass fractions. Given such strong starbursts, the distinction between the secondary-burst model and the primaeval-galaxy model then becomes somewhat semantic. For reasonable burst fractions, agreement seems unlikely, given the region defined by the distribution of the arcs on the colour–colour plane and the small time-scale during which the secondary-burst models enter this area. Neither the constant-SFR model nor the primaeval-galaxy model has such a grave problem with the time-scales. At $z=1$, both $B$ and $R$ are sampling the rest-frame ultraviolet, and may therefore be subject to strong reddening. To illustrate the upper limit on the possible role of dust, we plot in Fig. 1(b) the extinction vector for solar abundances.

For a subset of our sample, we have secured photometric data in a number of passbands and can thus construct spectral energy distributions which allow us to demonstrate the above result more clearly. The arcs with suitable data are Abell 370 A0, Abell 370 A5, Cl 0500−24 and Cl 2244−02, and we present their rest-frame SEDs in Fig. 4, together with those of the present-day Hubble sequence as would be observed at the redshift of the arc. As Aragón-Salamanca & Ellis (1990) showed, the giant arc A0 in Abell 370 ($z_{\rm arc}=0.72$) is fitted well by a normal spiral of class Sbc, but the higher redshift systems are clearly dominated by young stars, closely matching the SED of NGC 4449 – an intense star-forming system. Whilst the spectroscopic identifications for Abell 370 A5 and Cl 2244−02 remain somewhat uncertain, we stress that this redshift uncertainty does not significantly affect our conclusion about the nature of these sources, because the SED for the bluest Sdm/Irr classes maintains its shape more or less independently of redshift (cf. the flatness of the colour–redshift relations for NGC 4449 in Fig. 3).

### 4.2 Intrinsic luminosities and colour gradients

The gravitational magnification for the arcs in our sample is an issue central to the resolution of the question whether we are witnessing vigorous star formation in massive ($\simeq L^*$) systems or simply seeing individual star-forming clumps, either in isolation (e.g. as in the dwarf hypotheses discussed earlier) or as star-forming portions of normal galaxies.

In Table 2 the absolute $K$ luminosity of each arc has been estimated from its integrated apparent $K$ magnitude, assuming the spectroscopic redshift and an unresolved source with an intrinsic angular size equal to the seeing disc. This approach is justified in the discussion below. Since all are blue in colour, we determined a $k$-correction assuming a flat ($f_\nu\simeq$ constant) spectrum (Cowie et al. 1988). Where comparisons can be made, these magnifications agree with those calculated for individual arcs from detailed lensing geometries: magnification factors of $\sim 10$ are found. This tends to support the suggestion that the lensed galaxies are marginally sub-$L^*$ systems. The present-day remnants of these systems will depend critically upon their subsequent star formation histories. In the single-burst model they undergo purely passive evolution, leading to present-day counterparts with $M_K\sim -20$. If the constant-SFR model is valid and star formation continues at the same rate, then the final $z=0$ objects have $M_K\sim -25$.

Whereas it may ultimately be possible to derive quantitative estimates of the magnification by constraining the lensing geometry in clusters where there are a useful number of arcs and arclets (Tyson, Valdes & Wenk 1990; Smail 1993), another approach towards the resolution of this ambiguity is to search for colour gradients along the arcs. If the source is a highly magnified compact H II region (taking an extreme example) one might expect a remarkably uniform colour, whereas a more massive system might show a variation in colour, representative of resolved portions each exhibiting different star formation rates.

Unfortunately, measurement of reliable colour gradients is an exceedingly difficult task because of the inherent faintness of the sources and their location in the dense cluster cores. In the cases of Cl 0024+16 and the giant arc Abell 370 A0, no perceptible colour gradient is seen. A gradient might have been expected for the latter, given the earlier comments about its spectral energy distribution, but the situation is confused by a number of galaxies superimposed on this giant arc (Aragón-Salamanca & Ellis 1990). Aragón-Salamanca & Ellis measured colours in four uncontaminated regions and found no variations within their photometric errors. In the cases of Abell 370 A5 and Cl 0500−24, the $K$ signal is too faint for variations to be measured. Finally, for Abell 963, the northern arc is too embedded in the envelope of the cluster's cD galaxy and the southern arc has too low a surface brightness for a $K$ detection in the present data.

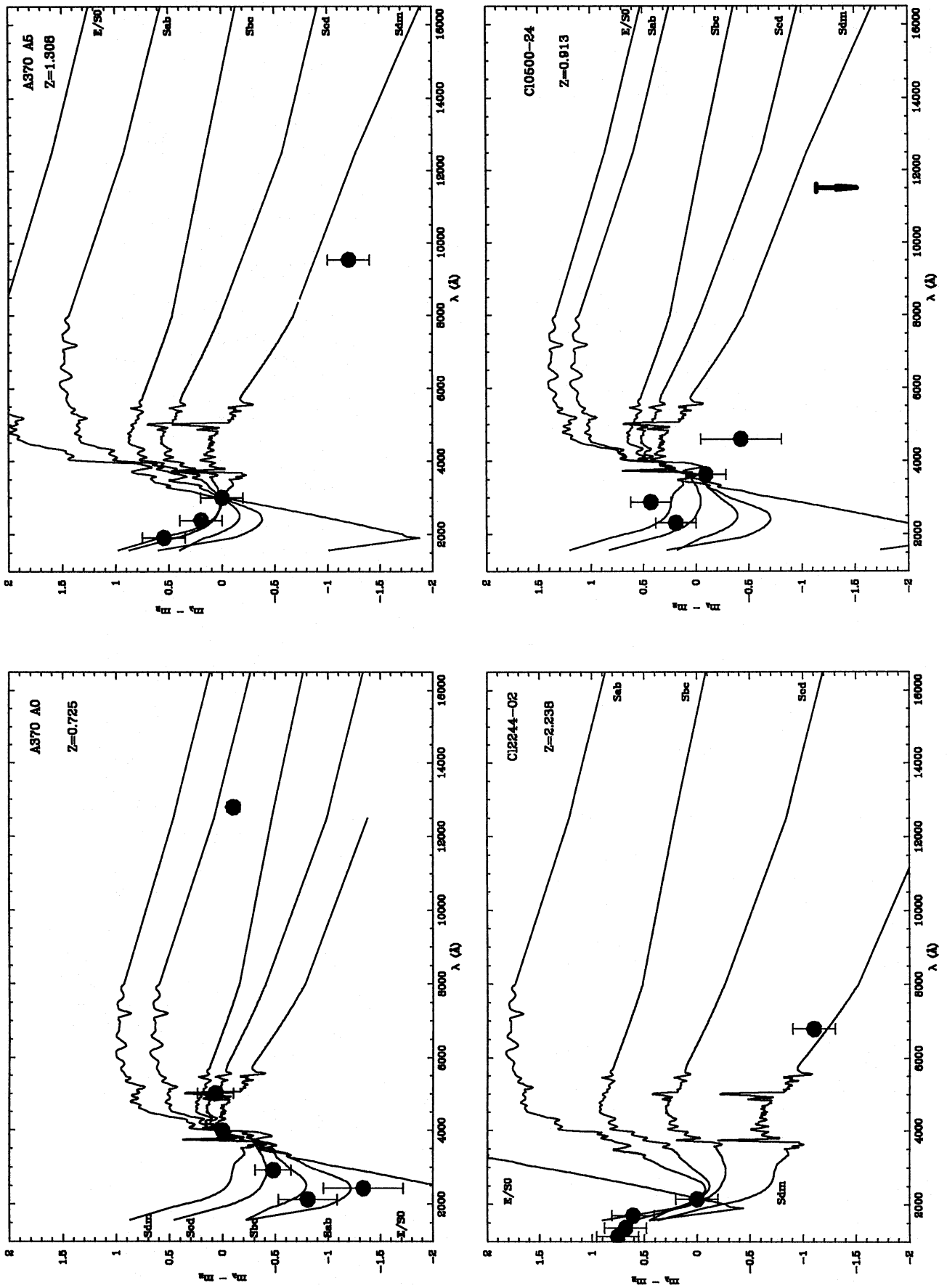


**Figure 4.** Spectral energy distributions for those arcs with extensive broad-band data. Data points are compared in the rest frame with the present-day Hubble sequence.

The only two arcs worthy of consideration for colour gradient studies are therefore Abell 2390 and Cl 2244−02. The former has probably the most reliable spectroscopic redshift ($z_{arc}=0.91$, Pelló et al. 1991), whereas the latter is representative of the star-forming high-redshift systems discussed above. Surface photometry and optical/optical–infrared colours as a function of position for these two cases are presented in Fig. 5. We discuss the two cases in turn.

#### 4.2.1 *Abell 2390*

The arc is surprisingly straight. Lensing geometries based on two potentials have been suggested by Pelló et al. (1991) and Blandford (1991), based on a strong velocity gradient of $\simeq 400$ km s$^{-1}$ seen in [O II] 3727 Å which is indicative of a massive star-forming system. Although this line is prominent across the entire arc, we find a striking optical–infrared colour gradient. Whereas the northern section shows a blue ($R-K=3.6\pm0.2$) colour representative of a spiral disc at $z_{arc}=0.91$, the southern region is substantially redder ($R-K=4.9\pm0.3$), as would be the case for an associated spheroidal component. Both sections of the arc are plotted in Fig. 1(a). The northern section is a member of the group of arcs which are blue in both optical and optical–infrared colours, while the southern section lies in a part of the plane occupied by old evolved populations that have superimposed young secondary star formation.

However, since there is no observed $B-R$ gradient, the likelihood of contamination from an unrelated very red source at the southern tip must be considered. The resolution of this paradox is not yet clear, because even the coolest M star would not distort the $R-K$ colour to the extent required without being visible as a source in the $B$ image. Another factor is the discrepant $B-R$ colour obtained by Mellier et al. (1991), noted earlier. Their optical colour, whilst not reproducible by us, would support the bulge + disc picture for a normal system at $z=0.91$.

Kassiola, Kovner & Blandford (1992) have suggested, on the basis of the velocity gradient data and stable lensing configurations, that *two* lensed sources may be involved. In this case, the similar $B-R$ colours of the two sources could result from a starburst induced by their interaction, while the different $R-K$ colours could reflect different pre-burst stellar populations. Higher resolution, deeper optical data are needed to make progress but, given our current information, this last explanation is the most consistent with the data.

#### 4.2.2 *Cl 2244−02*

Although the redshift of this arc is less well determined, the rising ultraviolet continuum does indicate a high redshift. Mellier et al. (1991) showed that, if the emission-line feature seen in their spectrum is Ly$\alpha$, its strength implies a high star formation rate per unit mass, consistent with the colours. Some structure is seen in the optical data (Fig. 2, opposite p. 632) and these variations have been modelled by Hammer & Rigaut (1991), who concluded that the arc comprises two images, with opposite parities, of a single face-on spiral galaxy, with surface brightness peaks corresponding to disc and bulge components. The $B-K$ colour variations show a symmetrical pattern across the break between the two proposed images, providing independent support for this lensing model.

In conclusion, therefore, of the four arcs with high enough signal-to-noise ratio to allow colour gradients to be detected, two show no gradient while the other two show strong gradients. In the latter cases, the gradients support the contention that the arc sources are reasonably massive systems which suffer moderate magnification.

## 5 DISCUSSION

There are two possible biases that may weaken the conclusions we can draw from our data set. First, given the difficulty of constraining the lensing magnifications from the internal photometric variations across the arcs, at least with the current data, we must rely on magnifications deduced from the arc sizes – this affects our derived source luminosities. Secondly, we recall the bias introduced earlier, arising from the fact that the arcs were all selected in blue optical passbands, which guarantees that star-forming systems will be found at high redshift. We now address these two concerns.

The intrinsic $K$ luminosities derived above imply that we are seeing sub-$L^*$ systems compared to objects at lower redshift. For a resolved arc, the axial ratio gives a good estimate of the magnification factor, the main uncertainties being the original source orientation and the core size of the lensing potential. Unfortunately, a majority of the arcs are unresolved, and this results in uncertain magnifications, as has recently been discussed by Hammer (1991) and Miralda-Escudé (1992). The ambiguity arises because, for a given radial distance from the centre of the lens, $r_{arc}$, the arc width depends upon both the original source dimensions and the core size of the lensing potential (Hammer 1991). For large elongations,

$$\frac{d_{arc}}{d_{source}} \propto \frac{1}{[1-\kappa(r_{core})]},$$

where $d_{arc}$ and $d_{source}$ are the arc and source widths, and $\kappa(r_{core})$ depends upon the mass surface density of the lens at the position of the arc. For a given arc position and cluster velocity dispersion $\sigma_{cl}$, the larger the core radius $r_{core}$, the larger the value of $\kappa$. The magnification, $A$, is given by

$$A \propto \frac{l_{arc}}{\pi d_{arc}} \frac{1}{[1-\kappa(r_{core})]^2}.$$

We can therefore propose two scenarios.

*Model 1*: a singular lens producing a moderate-magnification event ($A \sim l_{arc}/d_{arc}$) from a marginally unresolved source, $d_{source} \sim 1$ arcsec.

*Model 2*: a non-singular cluster lens with $r_{core} \sim 100$ kpc, giving a high magnification ($A \sim 5\, l_{arc}/d_{arc}$) with an intrinsically small source, $d_{source} \sim 0.1$ arcsec.

To distinguish between these two possibilities, we can draw upon two additional arguments: (i) we examine the angular sizes of faint unlensed sources; and (ii) we consider the implications of the lensing cross-section.

A large fraction of $B \leq 26$ sources appear resolved in good seeing; this is confirmed by preliminary results on the scale-

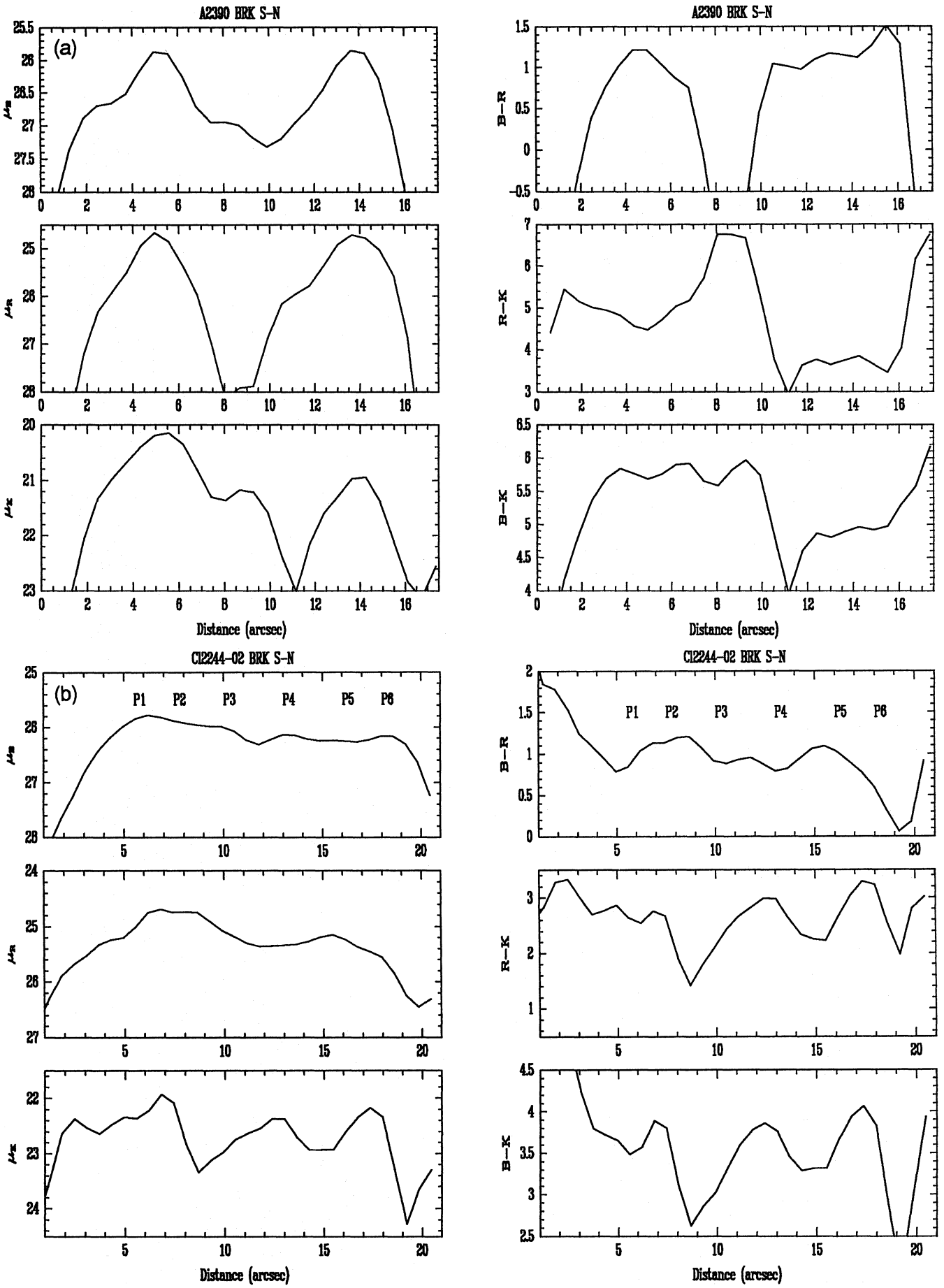


**Figure 5.** Surface brightness and colour profiles for the giant arcs in Cl 2244 − 02 and Abell 2390. The features marked for Cl 2244 − 02 refer to those discussed by Hammer et al. (1989). The profiles run from south to north along each arc.

sizes of faint galaxies from the *HST* Medium Deep Survey. This fact was used by Hammer (1991) to argue that the lensing potentials must be very compact if a typical giant arc has a $B=25$–$26$ source. Thus, if we assume that the lensing cluster potentials are close to singular, we have consistency between the predicted lensing magnifications, the source sizes and the magnitudes, with the sources being $B=25$–$26$ field galaxies. For the high-magnification model, however, the intrinsic source magnitude would lie fainter than the $B=26$ limit, where we have no knowledge of the source sizes. We can therefore only claim tentative support for model 1 from the self-consistency of the observations.

The probability of a high-magnification event ($A_c \gg 1$) is

$$P(A>A_c)\propto\frac{1}{A_c^2}$$

(Blandford & Kochanek 1987). If we require that the total galaxy mass, and hence $K$ luminosity, per unit volume be conserved with redshift (cf. Broadhurst et al. 1992) then we can derive a simple relation between luminosity, $L_i$, and space density, $N_i$, of sources at a given epoch for the two models: $N_1L_1=N_2L_2=$constant. We also have that $A_1L_1=A_2L_2=L_{arc}$. As the cross-section for the creation of a luminous arc in a particular model is given by the product of the space density of sources and the lensing probability, we have that

$$P(L_{obs}\geq L_{arc})\propto N_i\frac{1}{A_i^2}\propto\frac{1}{A_i}\propto L_i.$$

The probability of observing a bright arc therefore decreases as the source becomes fainter. It should be noted that this line of argument is not applicable to the optical observations, where the luminosity is seriously affected by the star formation and dynamical history. Although no complete sample of infrared-selected arcs has yet been constructed, the absence of small arcs of comparable surface brightness suggests support for model 1; indeed, for model 2 to be valid, the present surveys would have to miss the majority of intermediate-magnification arcs while finding only the most extreme events.

Although neither argument is particularly convincing, given the small sample size and possible selection biases, we conclude that the most likely scenario is that in which the sources are $B=25$–$26$ galaxies undergoing moderate magnification, supporting our earlier source luminosities. In Fig. 6(a) we compare the distribution of intrinsic source magnitudes and their absolute luminosities with those for the $B\leq24$, spectroscopic sample of Cowie et al. (1991), for which $K$ photometry is also available. A Kolmogorov–Smirnov (KS) test shows that there is a 12 per cent probability that the distributions of $M_K$ in the two samples are drawn from the same parent population. This drops to 2 per cent if we adopt the extreme-magnification model. This is equivalent to the statement that there is marginal evidence that the bright end of the $K$ luminosity function in our preferred model evolves between $B=22$–$24$ and $B\sim25$–$26$. This is seen as a slight trend to lower absolute luminosities at fainter magnitudes, in the direction expected under the merger hypothesis. This evolution is more apparent in the $M_K$–$z$ diagram (Fig. 6b), which shows an absence of

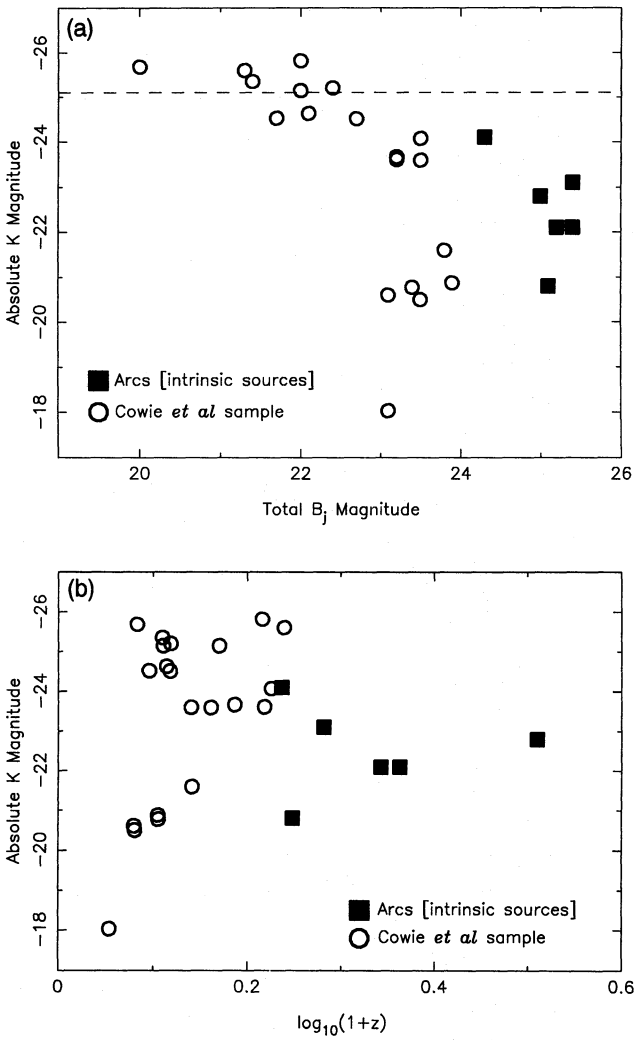


**Figure 6.** (a) $M_K$–$B$ diagram for the arc sample, together with that for the $B\leq24$ field sample of Cowie et al. (1991). The line shown is $M_K^*$ from a local field sample. (b) $M_K$–log$(1+z)$ plot showing the arc sources and the field sample of Cowie et al. (1991). There appears to be an absence of massive galaxies in the more distant arc sample compared to the distribution seen at $z\sim0.5$.

intrinsically bright galaxies in the arc sample compared to the distribution seen at lower redshift.

The present data set was not homogeneously selected, and in many ways does not resemble a normal magnitude-limited sample. In fact, it may be impossible to construct a well-defined sample, given the nature of the lensing process. More probably, arcs represent a *surface-brightness-limited* sample, similar to that of Smail et al. (1991). Such samples are prone to strong selection effects, as emphasized by Phillipps et al. (1990), in addition to problems associated with ultraviolet bias (see Section 2).

The most direct method of examining possible selection biases, at least in the optical–infrared colours of the arc sample, is to compare with a $K$-limited sample of faint field galaxies from the photometric survey of Cowie et al. (1988), which is statistically complete to $K=22$. Cowie et al. found the bulk of the $K$-selected galaxies to be blue and representative of those found to $B\simeq25$–$26$, i.e. there are few intrinsi-

cally red sources. A comparison of the $B-K$ colour distribution for the arcs and the field objects with $21<K<22$ shows agreement at the 99 per cent significance level using a two-sample KS test. In the event that a strong selection effect is at work in the arc sample, we might have expected our colour distribution to be skewed blueward. This gives us some confidence, notwithstanding the small sample size, that the arcs are no more biased towards extremely blue objects than is a normal field survey. The remaining problem with this argument is then the untypical colours of the only infrared-discovered arc, in Cl 2244−02. More examples are clearly needed to understand the significance of this particular object.

Although our two-colour plane (Fig. 1) argues against scenarios in which the blue arc colours are produced by secondary star formation in evolved galaxies, it has not been possible to distinguish directly between the models involving a primaeval burst and a more pedestrian history of continuous star formation. The absence of $z>1$ galaxies in the flat-spectrum field survey of Colless et al. (1993) is a strong argument against the former explanation. For example, in the primaeval-burst situation where the stars are formed $\sim 1$ Gyr before $z=1$, a galaxy with a culminating luminosity of $M_K\sim -23$ would reach an apparent $B$ magnitude at its most luminous phase of $B\sim 23$. The dearth of such galaxies in the Colless et al. (1993) survey is strong observational evidence against this picture. In the continuous star formation picture, the peak $B$ magnitude for equally blue sources can be arranged not to exceed $B\simeq 26$ (see also Baron & White 1987). Moreover, while the primaeval-burst model would require all the systems to be formed within $\sim 1$ Gyr of $z=1$ (i.e. $z\leq 1.5$), creating the possibility of a feature in the $B$ counts, the continuous star formation model allows a much more extended formation epoch while still being consistent with the distribution of arc colours.

The final observation to make is that the redshift distribution for the giant arcs is peaked at relatively low redshifts: ignoring the uncertain case of Cl 2244−02, 75 per cent lie below $z=1$. The low-redshift cut-off clearly arises because of the redshifts of the lensing clusters. The apparent lack of high-$z$ galaxies is, however, surprising. Although few high-$z$ sources are found in deep spectroscopic surveys to $B=24$, the equivalent result from the arc samples implies that, 2–3 mag fainter, we are still not uncovering a population of distant strongly evolving galaxies. Statistical tests, using the large population of slightly distorted arclets seen in rich clusters, support this conclusion (Smail 1993).

## 6 CONCLUSIONS

The main results and conclusions from our infrared photometry of a spectroscopic sample of giant arcs are summarized below.

(i) Giant arcs provide us with a unique and easily recognizable probe of the nature of field galaxies at high redshifts. Their optical–infrared colours are representative of galaxies found in the deepest field surveys. Although not yet constituting a statistically complete sample, their colour distribution shows no evidence of any bias arising from surface brightness or ultraviolet selection effects peculiar to the lensing process. As such, they can be regarded as a useful subsample of very faint field galaxies.

(ii) From a number of independent approaches, we show that the distribution of intrinsic luminosities of the arcs indicates that the sources are marginally less luminous in $K$ than a local field sample, as might be expected in the merger hypothesis. This evolution is apparent as a deficit of luminous galaxies in the arc sample compared to the $z\simeq 0.5$ field. Depending upon their subsequent star formation, these systems may appear as either faint red dwarf systems or large star-forming spirals at the present epoch.

(iii) The optical–infrared colours of the giant-arc sample show strong evidence for enhanced star formation. However, the blue colours cannot reasonably arise from secondary bursts superimposed upon pre-existing evolved systems. Neither can the star formation seen be a dramatic single event associated with galaxy formation. Such an event would render such sources visible in deep spectroscopic field surveys. More probably, we are witnessing an extended formation phase which continues to redshifts of at least $z\simeq 1$.

## ACKNOWLEDGMENTS

We thank PATT for generous support of the UKIRT arc programme over a number of semesters, and all the UKIRT staff, particularly Malcolm Smith and Tom Geballe, for their invaluable help in technical matters and in obtaining service exposures. We acknowledge cheerful assistance from the telescope operators Dolores Walther, Joel Aycock and Thor Wold. Mark Casali is thanked for writing data reduction software specifically to enable us to monitor our progress at the telescope. Useful discussions have been held with Simon Lilly, Len Cowie, Roger Blandford and David Koo. RSE and IS acknowledge financial support from the SERC. AAS acknowledges financial support from the Spanish Ministerio de Educación y Ciencia.

## REFERENCES

Aragón-Salamanca A., 1991, PhD thesis, Durham University
Aragón-Salamanca A., Ellis R. S., 1990, in Mellier Y., Soucail G., Fort B., eds, Gravitational Lensing. Springer-Verlag, p. 288
Aragón-Salamanca A., Ellis R. S., Sharples R. M., 1991, MNRAS, 248, 128
Babul A., Rees M. J., 1992, MNRAS, 255, 346
Baron E., White S. D. M., 1987, ApJ, 322, 585
Blandford R. D., 1991, QJRAS, 30, 305
Blandford R. D., Kochanek C. S., 1987, in Bahcall J., Piran T., Weinberg S., eds, Dark Matter in the Universe. World Scientific, Singapore, p. 133
Broadhurst T. J., Ellis R. S., Glazebrook K., 1992, Nat, 355, 55
Bruzual A. G., Charlot S., 1993, ApJ, 405, 538
Buzzoni A., 1989, ApJS, 71, 817
Colless M. M., Ellis R. S., Taylor K., Hook R. N., 1990, MNRAS, 244, 408
Colless M. M., Ellis R. S., Broadhurst T. J., Taylor K., Peterson B. A., 1993, MNRAS, submitted
Cowie L. L., Lilly S. J., Gardner J. P., McLean I. S., 1988, ApJ, 332, L29
Cowie L. L., Songaila A., Hu E. M., 1991, Nat, 354, 460
Elias J. H., Frogel J. A., Mathews K., Neugebauer G., 1982, AJ, 87, 1029
Ellis R. S., Allington-Smith J. R., Smail I., 1991, MNRAS, 249, 184
Fort B., 1990, in Mellier Y., Soucail G., Fort B., eds, Gravitational Lensing. Springer-Verlag, p. 221
Fort B., Prieur J. L., Mathez G., Mellier Y., Soucail G., 1988, A&A, 200, L17

Giraud E., 1992, preprint
Hammer F., 1991, ApJ, 383, 66
Hammer F., Rigaut F., 1991, A&A, 226, 45
Hammer F., Le Févre O., Jones J., Rigaut F., Soucail G., 1989, A&A, 208, L7
Kassiola A., Kovner I., Blandford R. D., 1992, ApJ, 396, 10
Koo D. C., 1988, in Rubin V. G., Coyne G. V., eds, Large-Scale Motions in the Universe. Princeton Univ. Press, Princeton, NJ, p. 513
McLean I. S., Chuter T. C., MacCaughrean M. J., Rayner J. T., 1985, Proc. SPIE, 627, 430
Mellier Y., Fort B., Soucail G., Mathez G., Cailloux M., 1991, A&A, 380, 334
Miralda-Escudé J., 1992, ApJ, 403, 497
Pelló R., Le Borgne J. F., Soucail G., Mellier Y., Sanajuja B., 1991, A&A, 366, 405
Phillipps S., Davies J. L., Disney M. J., 1990, MNRAS, 242, 235
Salpeter E. E., 1955, ApJ, 121, 161
Smail I., 1993, PhD thesis, Durham University
Smail I., Ellis R. S., Fitchett M. J., Nørgaard-Nielsen H. U., Hansen L., Jørgensen H. E., 1991, MNRAS, 252, 19
Soucail G., 1992, in Fabian A. C., ed., Clusters of Galaxies. Kluwer, Dordrecht, p. 199
Soucail G., Mellier Y., Fort B., Mathez G., Cailloux M., 1988, A&A, 191, L19
Tyson A. J., Valdes F., Wenk R. A., 1990, ApJ, 239, L1